Azimuthally polarized radial emission from a quantum dot fiber laser

Nan Zhang,[†,‡,▽] He Liu,[†,▽] Alexander M. Stolyarov,[§,∥] Ting Zhang,[†] Kaiwei Li,[†] Perry Ping Shum,[†,‡] Yoel Fink, [§] Xiao Wei Sun,*[,†,⊥] and Lei Wei*[,†,‡]

[†]School of Electrical and Electronic Engineering, Nanyang Technological University, 50 Nanyang Avenue, 639798, Singapore

[‡]CINTRA CNRS/NTU/THALES, UMI3288, Research Techno Plaza, 50 Nanyang Drive, 637553, Singapore

[§]Research Laboratory of Electronics, Massachusetts Institute of Technology, 77 Massachusetts Avenue, Cambridge, Massachusetts, 02139, USA

[⊥]Department of Electrical & Electronic Engineering, Southern University of Science and Technology, Shenzhen, 518055, China

ABSTRACT: We demonstrate an azimuthally polarized radial emission with zero-angular-momentum from a CdSe/CdZnS/ZnS quantum dots (QDs) fiber laser. This fiber laser is realized by axially pumping the QDs doped gain plug infiltrated in the hollow cavity of a multilayer photonic bandgap fiber. The cylindrically symmetric radial emission is registered as a perfect ring-shaped pattern in the far field. The lasing threshold is measured to be ~238 μJ/pulse and the quality factor (Q-factor) is calculated to be ~4000. The unique radial emission from the resulting QDs fiber laser offers a fundamental solution for the development of omnidirectional displays and light sources for biomedical analysis and phototherapy with minimal invasion.

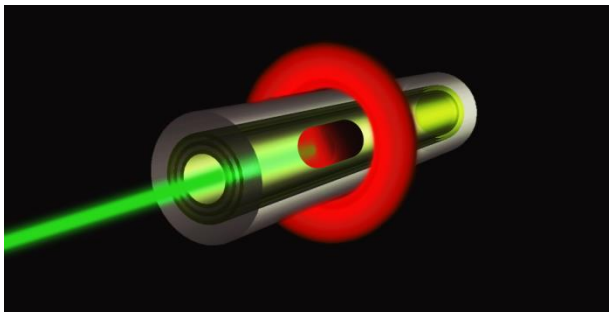

KEYWORDS: *Quantum Dots, Fiber Laser, Photonic Bandgap Fiber*

Optofluidic fiber lasers, which integrate aqueous gain medium and micrometer sized fiber cavities, have greatly contributed the development of miniaturized optical devices for integrated biomedical analysis systems, due to the characteristics of easy manipulation of liquid solutions, minimal invasion, low pump energy consumption, great compactness, and flexibility in the design of fiber cavity.[1–5] Depending on the fiber geometry and configuration, the laser can emit from the aqueous gain medium either along[6] or perpendicular[7,8] to the fiber axis. In particular, cylindrically symmetric laser emission in the transverse plane of the fiber axis is of great interest for the applications of omnidirectional imaging, biomedical detection and photodynamic therapy, providing extended laser emission surface area compared with the common fiber laser emission/guidance from a relatively small area along the fiber axis.[9,10] Conventional omnidirectional emission is realized by the excitation of whispering gallery modes (WGMs) at cavity boundary.[7] However, for WGM lasers, light escapes the fiber cavity through the diffraction or scattering at rough surface, resulting in a limit control over light output coupling. Besides, WGM is predominantly excited by a high power pump from the side, which brings more difficulties in real applications due to the complexity of the pump arrangement. To overcome these drawbacks and expand the applications of omnidirectional lasers, an in-fiber microfluidic cylindrically symmetric radial emission is demonstrated.[11] Nevertheless, the fast-bleaching of organic dyes limits the lasing performance under long exposure time, and further deteriorates in the laser cavity as both the pumping energy and emission intensity are high in the cavity.[12] In addition, the inherent optical properties of broad emission spectrum, narrow excitation band and being sensitive to ambient solvent conditions make organic dyes less applicable in constructing bio-analytical systems.[13,14]

Semiconductor quantum dots (QDs) have enabled intensive studies as alternatives to organic dyes in light emitting diodes (LEDs),[15] biosensing,[16,17] imaging[14,18] and versatile lasers,[19,20] providing their unique advantages of being less susceptible to photo-bleaching, great tunability over a wide spectra range, temperature insensitive lasing threshold, broad excitation band and narrow emission peaks.[12,21,22] In particular, their broad absorbance bands

allow the capability of simultaneous excitation of multi-color emission by exciting different QDs with single pumping wavelength. The narrow emission peaks of QDs, which have a typical full width at half maximum (FWHM) value of 20 to 30 nm , can be easily tuned from 400 nm to 2 μm by altering the size and material of QDs owing to the quantum confinement effect.[21] Furthermore, the characteristics of high absorption cross-section, high quantum yields and enhanced photochemical stability achieved with core/shell structured QDs contribute to construct robust and low threshold QDs lasers.[22–24] Given the premium benefits of QDs as gain medium and the flexibility of optofluidic fiber laser configurations, we demonstrate here the realization of a purely radial emission QDs fiber laser with fixed azimuthal polarization direction.

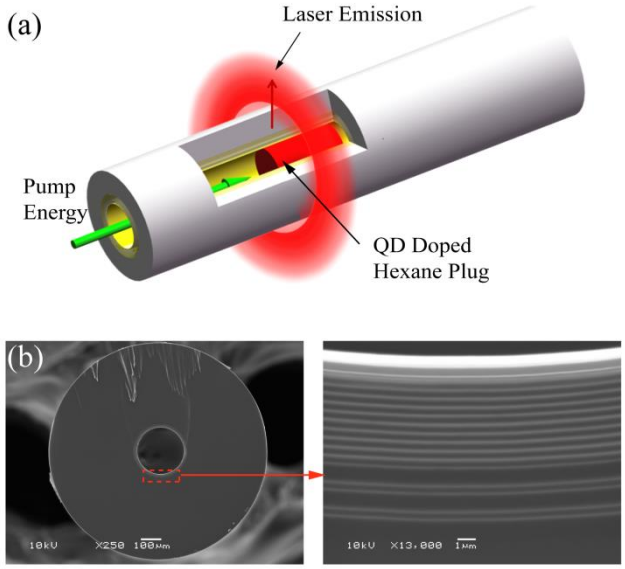

Figure 1. (a) Scheme of the laser emission; (b) SEM images of the PBG fiber.

The scheme of pump arrangement and the laser emission are shown in FIG. 1(a). The cylindrically symmetric laser emission is obtained by axially pumping the liquid gain medium in the hollow cavity of a photonic bandgap fiber (PBG) with a nanosecond Nd:YAG laser at 532 nm. Laser light is collected by a spectrometer from a direction perpendicular to the fiber axis. The multilayer PBG fiber in this experiment consists of a hollow air core surrounded by 25 annular alternating layers of high index chalcogenide glass ($As_{25}S_{75}$) and relatively low index polycarbonate (PC), and a pure PC cladding, as shown in scanning electron microscope (SEM) images in FIG. 1(b). The alternating high-index and low-index multilayers surrounding the hollow core impose a normal-incidence (axial wave vector equals to 0) band gap covering a broad wavelength range from 520 nm to 660 nm. The normal-incidence band gap provides necessary optical feedback for laser emission in the radial emission. Concurrently, the photonic bandgap structure of the hollow cavity is able to support an axial transmission band centered at 550 nm for optical pump (wave vector is in the axial direction). The inner diameter and outer diameter of the PBG fiber are measured to be around 250 μm and 1060 μm, respectively. To eliminate surface modes in the cavity, the multilayer geometry is ended with a layer of high index $As_{25}S_{75}$.

The QD used in this experiment is synthesized using 'one-pot' method[25] with modification. Both cadmium and zinc precursors ($Cd(OA)_2$ and $Zn(OA)_2$) are firstly made and heated to 300 °C. Selenium (Se) precursor is further injected with an optimized rate to form CdSe core. To cap CdSe core, alkyl thiol is used as sulfur (S) precursor to form CdZnS shell, and then trioctylphosphine dissolving S (TOPS) is added to produce ZnS shell. The resulting CdSe/CdZnS/ZnS QD has an emission centered at 636 nm and a FWHM value of ~ 30 nm, as shown in FIG. 2. The absorbance spectrum reveals that the resulting QD has a continuous absorption band below 650 nm and a larger absorbance to the shorter wavelength pump photons. The size of the QD is estimated to be 7 nm from the transmission electron microscopy (TEM) image shown in the inset of FIG. 2. A high quantum yield (QY) of 65% is obtained by exciting the QDs in hexane solution with 405 nm laser in an integrating sphere. All the characterizations are carried out at room temperature under ambient conditions. The high quantum yield is beneficial to reduce the lasing threshold which is essential in facilitating its practical applications.

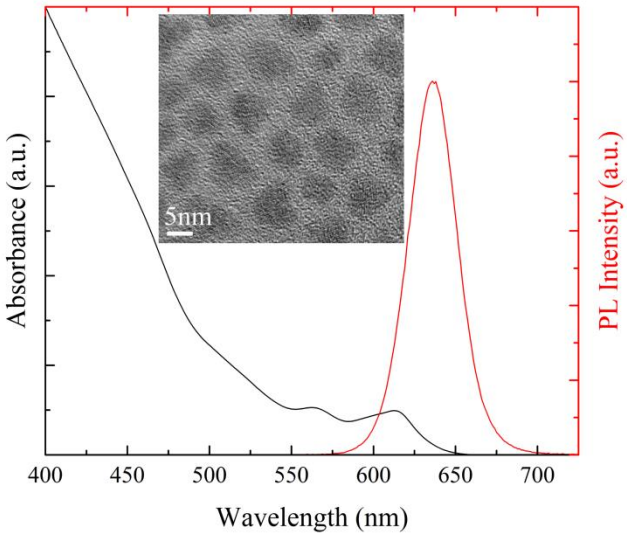

Figure 2. Absorbance and PL spectra of CdSe/CdZnS/ZnS QDs, and (inset) the TEM image of CdSe/CdZnS/ZnS QDs.

To start, a segment of QDs doped hexane solution (concentration: 100 mg/ml) is infiltrated into the hollow core of a 5-cm-long PBG fiber by capillary forces to act as the gain medium. A linearly polarized Nd:YAG laser with a pulse duration of ~5 ns is used to axially pump the gain medium. We observe that light emission from the fiber cavity is in the transverse plane to the fiber axis with cylindrical symmetry. The laser wavefront is registered as a perfect ring in the far field with the assistance of a paper funnel and a 550 nm long pass filter, as shown in the inset of FIG. 4. The cylindrical geometry of the laser emitted from is determined by the circular cross section of the fiber core and the penetration depth of the optical pump

in the gain medium instead of the actual length of the gain plug which is in the order of centimeters. In our experiment, the penetration depth for the 100 mg/ml QD hexane plug is ~ 500 μm. The cylindrically symmetric emission stems from the interplay between the isotropic fluorescence of QDs and the cylindrical fiber resonator. To characterize the omnidirectional output emission, we use a spectrometer (Ocean Optics, USB 2000) to collect the emission spectra under different pump pulse energies and plot them in FIG. 3. Each spectrum is collected at a single shot and an absorptive neutral density filter with an optical density of 1.3 is placed between the fiber and the spectrometer to avoid saturation. At low pump energy, the spectrum shows only broad band spontaneous emission of QDs. A narrow peak occurs above the longer wavelength range of the spontaneous emission band of the QDs when the pump pulse energy exceeds a specific value. The narrow emission peaks on the spectra confirm the lasing phenomenon and indicate that the isotropic spontaneous emission is coupled to specific low threshold laser modes supported by the cylindrical fiber resonator. The lasing threshold is estimated to be ~238 μJ/pulse by comparing the relationship between the peak intensities and pump pulse energies, as plotted in the inset of FIG. 3. Compared with dye molecule counterparts, this relatively larger laser threshold with QDs mainly results from their relatively low QY (the QY of R6G is normally above 90%[26]) and the competitive highly-efficient nonradiative Auger recombination[21] (AR) in QDs. The low QY of our QDs may be attributed to the unsaturated dangling bonds at the surface of QDs and defects at the core/shell interface. These defects act as traps for electrons or holes, which will increase the ratio of nonradiative decay. Besides, in strongly confined QDs, the highly-efficient AR dominates when the QDs are pumped under high-energy excited states, resulting in a limit on the gain lifetime and an increase of laser threshold. The threshold of our QD laser emission can be reduced by increasing the QY of QDs and suppressing the AR process through engineering the structure of QD interface.[27]

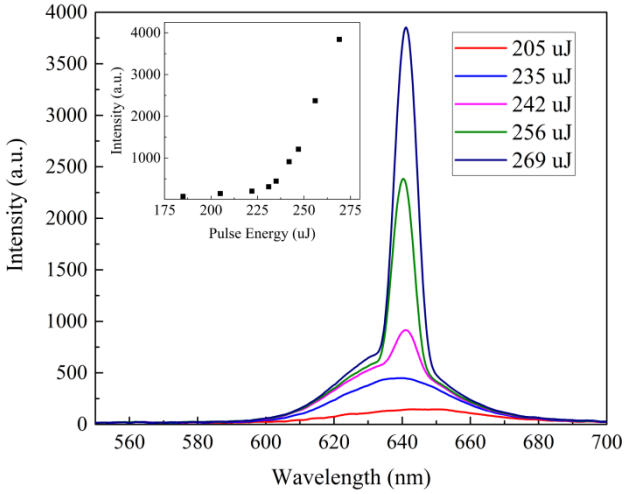

Figure 3. Spectra of radial emission from the laser cavity collected under different pump pulse energies, and (inset) the dependence of the peak intensity on the pulse energy.

To distinguish resonant laser peaks, we use a high resolution spectrometer (resolution: 0.11 nm) to collect the radial emission spectra at pump energies above the threshold. The distinct laser peaks in the spectra (FIG. 4) further verify the lasing phenomenon. The spacing between adjacent lasing peaks is measured to be around 0.58 nm for the fiber core with a diameter of ~250 μm. Given that, in a Fabry-Perot (F-P) cavity, the free spectral range (FSR) of longitudinal modes is calculated by the formula, $FSR = \lambda_0^2/2nd$, where λ_0 is the wavelength of central lasing peak (λ_0 = 642 nm) and n represents the refractive index (RI) of the gain medium plug (n = 1.3749), the diameter of the fiber cavity (d) is therefore calculated to be ~258 μm, which matches well with the actual size of our fiber cavity. The calculation result reveals that the lasing mode is occupied by the photons propagating along the radial direction. To further prove the laser cavity, we simulate the transmission spectral response of this PBG hollow cavity with FDTD solutions and obtain a theoretical FSR of 0.59 nm which agrees with our experimental results, and a theoretical Q-factor of ~7000 near 642 nm . In the experiments, the FWHM value (Δλ) of individual lasing peak is approximately 0.16 nm, indicating a high quality factor (Q-factor) of ~4000 ($Q = \lambda_0/\Delta\lambda$). The slight deviation in the Q-factor value is acceptable taking into consideration that the condition of the PBG structure of the fabricated fiber is less possibly as ideal as in the simulation, the effect of the optical property of the gain medium and as well as the resolution of spectrometer. This Q-factor value is one order of magnitude higher than the dye doped counterpart,[11] indicating a more promising lasing performance engaged with QDs gain medium.

To characterize the polarization state of the laser emission, we analyze the intensity variation of the output laser with different polarization angles under a fixed pump energy. The measurements are carried out by rotating a linear polarizer placed in-between the fiber and a spectrometer. The scheme is illustrated in the inset of FIG. 5, where the blue arrows on the fiber indicate the direction of transmission axis of the polarizer, and the intensity is normalized to the maximum intensity collected. We assume that the polarization angle equals to 0 when the transmission axis of the polarizer is perpendicular to the fiber axis. The measured laser intensities against polarization angles are plotted in FIG. 5. The dependence of the laser intensity on the polarization angle fit well with a cosine-square function, demonstrating that the radial laser emission is dominantly azimuthally polarized. This phenomenon confirms that the isotropic spontaneous emission is coupled to high Q-factor low threshold TE_{on} modes with the same electric field polarization state as obtained from this laser emission.

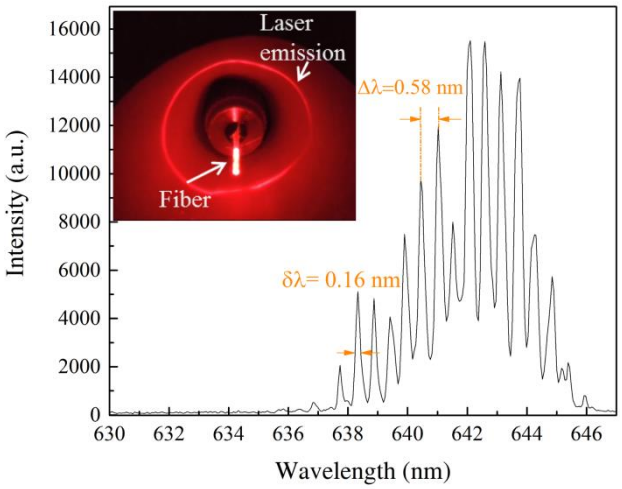

Figure 4. High resolution spectrum of the radially emitted QD fiber laser collected at pump energy above the lasing threshold, and (inset) the wavefront of the laser emission in the far field.

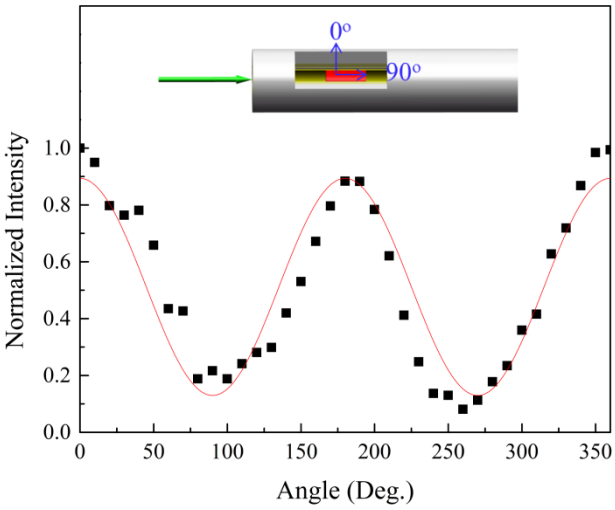

Figure 5. Dependence of the output intensity on the polarization angle. The black squares are measured data, and the red curve fits to the experimental data with a cosine-square function. Inset: the scheme of the polarization measurements. The blue arrows label the directions of transmission axis of the polarizer placed in-between the fiber and a spectrometer.

In conclusion, we demonstrate a QD fiber laser with azimuthally polarized radial emission. The laser is realized by axially pumping the CdSe/CdZnS/ZnS QDs doped hexane plug in the hollow cavity of a PBG fiber using a nanosecond Nd:YAG laser at 532 nm. The cylindrically symmetric radial emission results from the isotropic fluorescence of QDs and its coupling to low-threshold TE_{on} modes. The laser emission exhibits a threshold of ~238 μJ/pulse and a high Q-factor of ~4000. As the PL spectrum of CdSe/CdZnS/ZnS QDs performs relatively good stability around room temperature,[28] the fiber laser can work well as long as we avoid using ultrahigh-energy pump pulse that can boil the hexane solvent. The resulting laser platform integrates the advantages of QDs as gain medium and the unique emission characteristics and remote pumping, providing a substantial impact on both studies of lasing mechanism and future developments of a variety of applications. The ability to provide large area cylindrical symmetric laser emission, combined with ultrasonic circular-array detectors, will enable photoacoustic computed tomography (PACT) systems to generate full-view and high quality images in round objects with fast data acquisition speed.[29] In a similar way, our fiber laser could be integrated into photoacoustic endoscopy (PAE) systems to provide much convenience for the application of circumferential cross-sectional scanning. Besides, taking into consideration of the characteristics of large wavelength tenability and broad absorption band of QDs, this fiber laser can serve as a flexible optical pump for activating various kinds of molecules for detection or diagnosis of diseases in vessel structures, or in conjunction with drugs to realize photo dynamic therapy. Finally, the convenient pump arrangement and extended laser emission surface make this fiber laser suitable for constructing omnidirectional or textile fabric displays.

AUTHOR INFORMATION

Corresponding Author

*E-mail (Lei Wei):WEI.LEI@ntu.edu.sg
*E-mail (Xiao Wei Sun):EXWSun@ntu.edu.sg

Notes

The authors declare no competing financial interest.

Present Addresses

‖Current address (Alexander M. Stolyarov): MIT Lincoln Laboratory, Massachusetts Institute of Technology, 244 Wood St., Lexington, Massachusetts 02420, USA

Author Contributions

▽These authors (Nan Zhang and He Liu) contributed equally.

ACKNOWLEDGMENT

We acknowledge the financial support from Singapore Ministry of Education Academic Research Fund Tier 2 (MOE2015-T2-1-066, MOE2015-T2-2-010, and MOE2014-T2-1-076), National Research Foundation, Prime Minister's Office, Singapore under its Competitive Research Programme (NRF-CRP11-2012-01), NRF-ANR Joint Grant (NRF2015-NRF-ANR000-MULHYN), NTU Research Student Scholarship (RSS), and Nanyang Technological University (Startup grant: Lei Wei).

REFERENCES

(1) Fan, X.; Yun, S.-H. The Potential of Optofluidic Biolasers. *Nat. Methods* **2014**, *11* (2), 141–147.

(2) Li, Z.-L.; Liu, Y.-G.; Yan, M.; Zhou, W.-Y.; Ying, C.-F.; Ye, Q.; Tian, J.-G. A Simplified Hollow-Core Microstructured Optical Fibre Laser with Microring Resonators and Strong Radial Emission. *Appl. Phys. Lett.* **2014**, *105* (7), 71902.

(3) Schmidt, H.; Hawkins, A. R. The Photonic Integration of Non-Solid Media Using Optofluidics. *Nat. Photonics* **2011**, *5* (10), 598–604.

(4) Zhang, X.; Lee, W.; Fan, X. Bio-Switchable Optofluidic Lasers Based on DNA Holliday Junctions. *Lab Chip* **2012**, *12* (19), 3673–3675.

(5) Russell, P. Photonic Crystal Fibers. *Science (80-.).* **2003**, *299* (5605), 358–362.

(6) Gerosa, R. M.; Sudirman, A.; Menezes, L. de S.; Margulis, W.; de Matos, C. J. S. All-Fiber High Repetition Rate Microfluidic Dye Laser. *Optica* **2015**, *2* (2), 186–193.

(7) Shopova, S. I.; Zhou, H.; Fan, X.; Zhang, P. Optofluidic Ring Resonator Based Dye Laser. *Appl. Phys. Lett.* **2007**, *90* (22), 2005–2008.

(8) Moon, H. J.; Chough, Y. T.; An, K. Cylindrical Microcavity Laser Based on the Evanescent-Wave-Coupled Gain. *Phys. Rev. Lett.* **2000**, *85* (15), 3161–3164.

(9) Shapira, O.; Kuriki, K.; Orf, N. D.; Abouraddy, A. F.; Benoit, G.; Viens, J. F.; Rodriguez, A.; Ibanescu, M.; Joannopoulos, J. D.; Fink, Y.; Brewster, M. M. Surface-Emitting Fiber Lasers. *Opt. Express* **2006**, *14* (9), 3929–3935.

(10) Zhang, N.; Humbert, G.; Gong, T.; Shum, P. P.; Li, K.; Auguste, J.-L.; Wu, Z.; Hu, D. J. J.; Luan, F.; Dinh, Q. X.; Olivo, M.; Wei, L. Side-Channel Photonic Crystal Fiber for Surface Enhanced Raman Scattering Sensing. *Sensors Actuators B Chem.* **2016**, *223*, 195–201.

(11) Stolyarov, A. M.; Wei, L.; Shapira, O.; Sorin, F.; Chua, S. L.; Joannopoulos, J. D.; Fink, Y. Microfluidic Directional Emission Control of an Azimuthally Polarized Radial Fibre Laser. *Nat. Photonics* **2012**, *6* (4), 229–233.

(12) Kiraz, A.; Chen, Q.; Fan, X. Optofluidic Lasers with Aqueous Quantum Dots. *ACS Photonics* **2015**, *2*, 707–713.

(13) Alivisatos, A. P.; Gu, W.; Larabell, C. Quantum Dots as Cellular Probes. *Annu. Rev. Biomed. Eng.* **2005**, *7* (1), 55–76.

(14) Resch-Genger, U.; Grabolle, M.; Cavaliere-Jaricot, S.; Nitschke, R.; Nann, T. Quantum Dots versus Organic Dyes as Fluorescent Labels. *Nat. Methods* **2008**, *5* (9), 763–775.

(15) Caruge, J. M.; Halpert, J. E.; Wood, V.; Bulovic, V.; Bawendi, M. G. Colloidal Quantum-Dot Light-Emitting Diodes with Metal-Oxide Charge Transport Layers. *Nat. Photonics* **2008**, *2*, 247–250.

(16) Sutter, J. U.; Birch, D. J. S.; Rolinski, O. J. The Effect of Intensity of Excitation on CdSe/ZnS Quantum Dots: Opportunities in Luminescence Sensing. *Appl. Phys. Lett.* **2011**, *98* (2), 1–4.

(17) Xiao, Y.; Barker, P. E. Semiconductor Nanocrystal Probes for Human Chromosomes and DNA. *Minerva Biotecnol.* **2004**, *16* (4), 281–288.

(18) Huang, F. M.; Festy, F.; Richards, D. Tip-Enhanced Fluorescence Imaging of Quantum Dots. *Appl. Phys. Lett.* **2005**, *87* (18), 1–3.

(19) Schäfer, J.; Mondia, J. P.; Sharma, R.; Lu, Z. H.; Susha, a. S.; Rogach, a. L.; Wang, L. J. Quantum Dot Microdrop Laser. *Nano Lett.* **2008**, *8* (6), 1709–1712.

(20) Wang, Y.; Leck, K. S.; Ta, V. D.; Chen, R.; Nalla, V.; Gao, Y.; He, T.; Demir, H. V.; Sun, H. Blue Liquid Lasers from Solution of CdZnS/ZnS Ternary Alloy Quantum Dots with Quasi-Continuous Pumping. *Adv. Mater.* **2015**, *27*, 169–175.

(21) Klimov, V.; Mikhailovsky, A.; Xu, S.; Malko, A.; Hollingsworth, J.; Leatherdale, C. A.; Eisler, H.; Bawendi, M. G. Optical Gain and Stimulated Emission in Nanocrystal Quantum Dots. *Science (80-.).* **2000**, *290* (5490), 314–317.

(22) Wang, Y.; Fong, K. E.; Yang, S.; Ta, V. D.; Gao, Y.; Wang, Z.; Nalla, V.; Demir, H. V.; Sun, H. Unraveling the Ultralow Threshold Stimulated Emission from CdZnS/ZnS Quantum Dot and Enabling High-Q Microlasers. *Laser Photon. Rev.* **2015**, *9* (5), 507–516.

(23) Dabbousi, B. O.; Rodriguez, J.; Mikulec, F. V; Heine, J. R.; Mattoussi, H.; Ober, R.; Jensen, K. F.; Bawendi, M. G. (CdSe)ZnS Core - Shell Quantum Dots : Synthesis and Characterization of a Size Series of Highly Luminescent Nanocrystallites. *J. Phys. Chem. B* **1997**, *101* (97), 9463–9475.

(24) Lin, C. H.; Lafalce, E.; Jung, J.; Smith, M. J.; Malak, S. T.; Aryal, S.; Yoon, Y. J.; Zhai, Y.; Lin, Z.; Vardeny, Z. V.; Tsukruk, V. V. Core/Alloyed-Shell Quantum Dot Robust Solid Films with High Optical Gains. *ACS Photonics* **2016**, *3* (4), 647–658.

(25) Ki Bae, W.; Kwak, J.; Lim, J.; Lee, D.; Ki Nam, M.; Char, K.; Lee, C.; Lee, S. Multicolored Light-Emitting Diodes Based on All-Quantum-Dot Multilayer Films Using Layer-by-Layer Assembly Method. *Nano Lett.* **2010**, *10* (7), 2368–2373.

(26) Magde, D.; Wong, R.; Seybold, P. G. Fluorescence Quantum Yields and Their Relation to Lifetimes of Rhodamine 6G and Fluorescein in Nine Solvents: Improved Absolute Standards for Quantum Yields. *Photochem. Photobiol.* **2002**, *75* (4), 327–334.

(27) Bae, W. K.; Padilha, L. A.; Park, Y.; Mcdaniel, H.; Robel, I.; Pietryga, J. M.; Klimov, V. I. Controlled Alloying of the Core Â Shell Interface in CdSe / CdS Quantum Dots for Suppression of Auger Recombination. *ACSNano* **2013**, *7* (4), 3411–3419.

(28) Jing, P.; Zheng, J.; Ikezawa, M.; Liu, X.; Lv, S.; Kong, X.; Zhao, J.; Masumoto, Y. Temperature-Dependent Photoluminescence of CdSe-Core CdS/CdZnS/ZnS- Multishell Quantum Dots. *J. Phys. Chem. C* **2009**, *113* (31), 13545–13550.

(29) Wang, L. V.; Hu, S. Photoacoustic Tomography: In Vivo Imaging from Organelles to Organs. *Science (80-.).* **2012**, *335* (6075), 1458–1462.

For Table of Contents Only